Effect of nonlocality on sub-barrier fusion enhancement

S. V. S. Sastry, A. K. Mohanty, and S. K. Kataria
Nuclear Physics Division, Bhabha Atomic Research Centre, Bombay 400085, India
(Received 18 December 1996)

The effect of nonlocality on heavy ion fusion is discussed at sub-barrier energies. It is shown that a simple barrier penetration model with a nonlocal ion-ion potential cannot reproduce the coupled channel results, though it gives rise to fusion enhancement at low energies. It is further shown that the coupled channel effects are important for fusion around the Coulomb barrier energies whereas the nonlocal effects give a large cross section enhancement at deep sub-barrier energies. [S0556-2813(97)06008-1]

PACS number(s): 25.70. Jj, 24.10.Eq

I. INTRODUCTION

It is well known that the enhancement of the fusion cross sections and the broadening of fusion spin distributions at sub-barrier energies cannot be explained on the basis of a simple one-dimensional barrier penetration model (BPM) [1]. Recently Galetti *et al.* [2] showed the importance of the nonlocal part of the ion-ion potential, which was not considered earlier in the BPM calculations. This nonlocal part has been implemented in a phenomenological way in the BPM calculations [2]. The presence of the nonlocality modifies the kinetic energy part of the Hamiltonian through the reduced mass which has a lower value up to the barrier position (R_b) and it resumes its normal value beyond R_b [2]. Using this approach, Galletti *et al.* and more recently Dutt *et al.* [3] tried to explain the large enhancements in fusion cross sections in the sub-barrier region for a number of systems. In all these calculations, the effective reduced mass was expanded in terms of the nonlocal parameter up to second order. However, this expansion is not valid for large values of the nonlocal parameter, often found necessary to fit the experimental fusion data [2,3]. Using the same approach, we report in this paper that we are not able to fit the observed fusion cross sections. Further, we found that the large enhancements as reported in [2,3] are an artifact of the parabolic approximation made for the reduced mass. We have also shown that the model of Galetti *et al.* is very much similar to the effective fusion barrier (EFB) model of Sahu and Shastry [4], though they differ in their interpretation. In both these models, the barrier height is reduced up to a certain radius, as if the ion-ion potential were more attractive in the nuclear interior region. We have shown that although these models can give fusion cross section enhancement, but they cannot reproduce the dynamical effects of the coupled channel (CC) calculations, particularly around the barrier region. The channel coupling effects are important around the Coulomb barrier energies whereas the nonlocal effects give large enhancement for cross sections at deep sub-barrier energies. In a consistent approach, CC calculations have also been carried out with the inclusion of nonlocal ion-ion potential.

II. BARRIER PENETRATION MODEL WITH NONLOCAL ION-ION POTENTIAL

The nonlocality arises from many-body quantum effects and reflects the fundamental nature of the nucleus-nucleus potential. In [2], Galetti *et al.* have introduced these nonlocal effects in a phenomenological way by using an effective Hamiltonian given by

$$H(p,r;b)\approx \frac{p^2}{2\mu g(r,b)}+V(r). \tag{1}$$

Here $V(r)$ can be identified as the local part of the standard ion-ion potential with Coulomb and centrifugal parts. Further, $g(r,b)$ in Eq. (1) is the nonlocal factor which modifies the reduced mass μ to μ' $[\mu'=\mu g(r,b)]$ in the kinetic energy part of the Hamiltonian as given by

$$g(r,b)=\left(1+\frac{\mu b^2}{2\hbar^2}\left|V^0(r)\right|\right)^{-1}. \tag{2}$$

$V^0(r)$ in Eq. (2) is the zeroth moment of the nonlocal ion-ion potential and will be identified as the standard attractive potential $V_N(r)$. With this definition, the WKB approximation for the transmission through the barrier can be written as

$$T_l(E,b)=[1+e^{2S}]^{-1}, \tag{3}$$

where S is the action defined by

$$S=\int_{r_1}^{r_2}\sqrt{\frac{2\mu g(r,b)}{\hbar^2}[V_l(r)-E]}\,dr. \tag{4}$$

Though $\mu g(r,b)$ in Eq. (4) can be treated as an effective reduced mass $\mu'(r,b)$, we treat this $g(r,b)$ factor separately. It is to ensure that this effect is present in the kinetic energy terms only and not in the centrifugal potential which also involves reduced mass. Therefore, the centrifugal part of the potential is given by $l(l+1)\hbar^2/2\mu r^2$, with the normal value of μ. Further following [2], $g(r,b)$ is approximated as

$$\begin{aligned} g(r,b)&=1 \quad \text{for } r>R_b \\ &=\frac{1}{1+b^2 f(R_b)} \quad \text{for } r\leqslant R_b, \end{aligned} \tag{5}$$

where R_b is the barrier position and $f(R_b)=\mu|V_N(R_b)|/(2\hbar^2)$. It is clear from the Eq. (5) that the nonlocal part of the nucleus-nucleus potential gives a partial reduction of the reduced mass, leading to an enhancement in

the transmission coefficient. In this description, the reduced mass is also dependent on the nonlocal range parameter b. Under the parabolic barrier approximation, the action S can be written as

$$S=\frac{2\pi}{\hbar\omega}\frac{1+\sqrt{g}}{2}(V_l-E), \tag{6}$$

where

$$V_l=V_0+\frac{l(l+1)\hbar^2}{2\mu r^2}. \tag{7}$$

It can be seen from the above equation that for $b=0$, there are no nonlocal effects, i.e., the g factor becomes unity and the effective mass is the same as the normal reduced mass. However, the nonlocal effects enhance the transmission through the value of $\hbar\omega$ that increases by a factor of $2/(1+\sqrt{g})$, thereby effectively making the barrier thin. It can be seen that this factor has a maximum value of 2, corresponding to the maximum nonlocal correction given by $g=0$. In other words, the action S cannot be reduced to value less than $(\pi/\hbar\omega)(V_l-E)$. For very small values of b, the factor $(1+\sqrt{g})/2$ can be approximated up to second order given by $(1-b^2f/4)$ as used in [2,3]. The use of this approximation can not be extended to large values of b which can result in spuriously large value of $\hbar\omega$, whereas this factor cannot exceed twice its normal value.

Now using Eqs. (3)–(5) for transmission, fusion cross section can be written as

$$\sigma(E,b)=\frac{\pi}{k^2}\sum_l (2l+1)T_l(E,b). \tag{8}$$

In the following we consider four typical heavy ion systems, i.e., ^{16}O+ ^{154}Sm, ^{28}Si+ ^{154}Sm, ^{58}Ni+ ^{64}Ni, and ^{19}F+ ^{232}Th. In the case of the ^{16}O+ ^{154}Sm system, the Sm target is strongly deformed. In addition, precise measurements of the fusion cross sections [5] and the average spin values [6] are also available over a wide range of energies. In the case of ^{28}Si+ ^{154}Sm, in addition to the rotational states of Sm, one has to consider an oblate deformation of Si with β_2 value of ≈ -0.41. This combination not only gives a large enhancement of the fusion cross sections, but also shows a pronounced bump in the average spin values around the barrier region [7], which is a characteristic feature of strong channel couplings. The ^{58}Ni+ ^{64}Ni system has several low lying inelastic levels in addition to the $2n$ transfer channel which plays a dominant role in enhancing fusion cross sections at sub-barrier energies [8]. We also consider a fissile system of ^{19}F+ ^{232}Th, which shows large fusion cross section enhancement at deep sub-barrier energies [9]. Figures 1–4 show the experimental and estimated fusion cross sections for these heavy ion systems. In these calculations, we have used Christensen-Winther parametrization for ion-ion potential [10]. However, the barrier height has been adjusted slightly to fit the above barrier cross sections. The long-dashed curve shows the simple BPM results without any nonlocal corrections. In Refs. [2,3], the nonlocal parameter b was varied between 1.6 fm and 2.3 fm while f was estimated from the

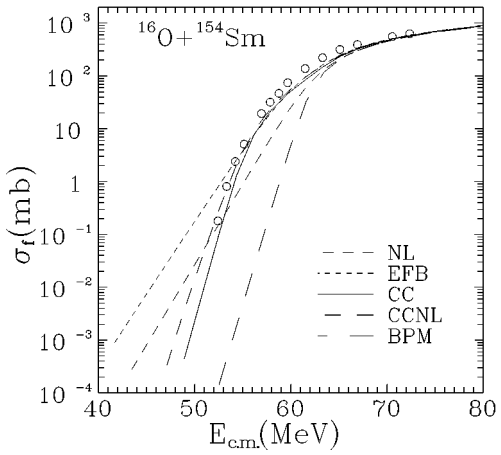

FIG. 1. Fusion excitation function and the average spin as a function of energy for ^{16}O+ ^{154}Sm system. The curves labeled NL and EFB are the predictions of BPM with nonlocal effects with $R_f=R_b$ (NL) and R_f adjusted to fit the data (EFB). The curve labeled CC represents the CCFUS results. The static deformation parameters used are $\beta_2=0.34$, $\beta_4=0.07$ for Sm and a 3^- state of O with $\beta=0.301$ with a Q value of -6.13 MeV. The other parameters are $V_b=61.48$ MeV, $R_b=10.88$ fm, and $\hbar\omega=4.4$ MeV. The curve CCNL represents the CCFUS calculations with inclusion of nonlocal effects. The experimental data points are taken from Refs. [5,6]. The curve labeled BPM in all these figures refers to the one-dimensional barrier penetration model results.

nuclear potential $V_N(r)$ at $r=R_b$. In general, f is a function of r and one should use an average value, $\langle f\rangle$, between $f(r_1)$ and $f(R_b)$. Therefore, the effective nonlocal factor b^2f in Eq. (5) can be very large and consequently, the contribution to the action integral in Eq. (4) from r_1 to R_b can be neglected as compared to the contribution from R_b to R_2. In order to maximize the effect of nonlocality, we take a very large value for the $b_{\rm eff}$ ($b_{\rm eff}=b^2\langle f\rangle$) parameter. The corresponding results for fusion cross sections are shown in Figs. 1–4 by the curves labeled NL. It may be mentioned here that we use a large $b_{\rm eff}$ parameter in order to estimate an upper bound on the enhancements of the cross sections.

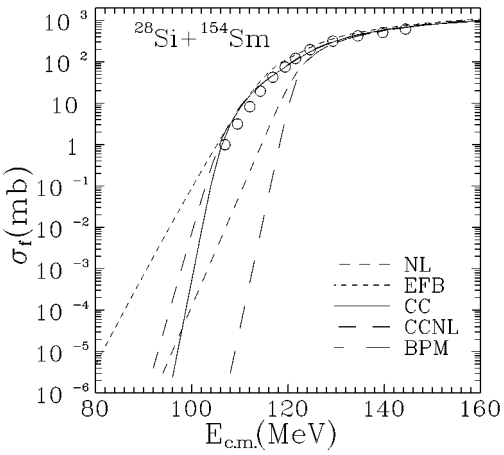

FIG. 2. Same as Fig. 1, but for the ^{28}Si+ ^{154}Sm system. The deformation parameters for Sm are the same as for Fig. 1 and the β_2 =-0.41 for Si . The barrier parameters are $V_b=102.26$ MeV, $R_b=11.47$ fm, and $\hbar\omega=4.24$ MeV. The experimental data points are taken from Refs. [7,13].

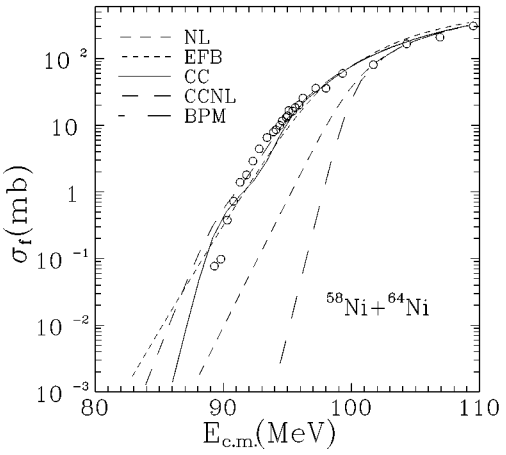

FIG. 3. The same as Fig. 1, but for the ^{58}Ni+^{64}Ni system. The coupling parameters for CCFUS calculations are taken from Ref. [8] which include 2^+, 3^-, and 4^+ states and also the transfer channels. The barrier parameters are V_b=99.46 MeV, R_b=10.54 fm, and $\hbar\omega$=3.529 MeV. The experimental data points are taken from Ref. [8] and the references therein.

The results for the ^{16}O+^{154}Sm system may be directly compared with the calculations of Dutt *et al.* [3]. In their work, instead of using a parabolic approximation to the barrier, they calculated the transmission exactly and concluded that the fusion enhancement is not enough to explain the experimental data. However, their estimates are much higher than our results for the same system. The curve *NL*, shown in the figure for this system, is an upper limit for nonlocal effects as we have used a parabolic barrier approximation as well as a very large value of $b_{\rm eff}$ parameter, corresponding to $g\approx 0$. It is also important to note that the maximum enhancement due to the nonlocal BPM calculations as suggested by Galetti *et al.* is far less than the experimental estimates. This discrepancy is more when the systems are strongly coupled to various rotational and vibrational states (see Fig. 2 and Fig. 3). We can conclude from these calculations that if nonlocal effects are included properly in BPM, the fusion enhancement is much less than the corresponding experimental values even for the case of $g\approx 0$. Therefore, the large enhancements found by Galetti *et al.* and also by Dutt *et al.* are a result of the approximations made in the expansion of the reduced mass.

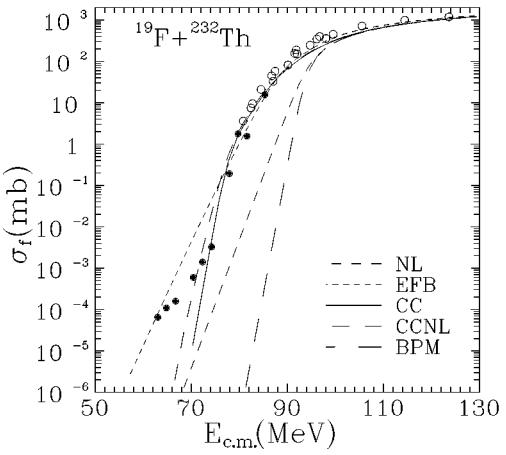

FIG. 4. The same as Fig. 1, but for the ^{19}F+^{232}Th system. The coupling parameters include the 3^- state of ^{19}F with $Q=-6.13$ MeV, β_2=0.301 and β_2 =0.22, β_4=0.09 for Th. The barrier parameters are V_b=90.93 MeV, R_b=11.71 fm, and $\hbar\omega$=4.67 MeV. The experimental data points are taken from Refs. [9,12].

It is interesting to note here that in an earlier work, Sahu and Shastry had also found similar results by using an effective fusion barrier model (EFB) [4]. In their work they had set the potential to zero inside some effective fusion radius (R_f) as follows:

$$V(r)=0 \quad \text{for } r<R_f. \tag{9}$$

Therefore, they calculated the transmission only from R_f to the outer turning point R_2, where R_f was taken as a parameter to be fixed by fitting the fusion data. They found the R_f value to be larger than the R_b value for many systems. The present work with maximum nonlocal effects (i.e., $g\approx 0$) and the effective fusion barrier model of Ref. [4] with $R_f=R_b$ are in a way similar, although the authors in Ref. [4] did not interpret their results in terms of the nonlocal effects explicitly. In the following, we also calculate the fusion cross sections using the EFB model of Sahu and Shastry, where R_f is treated as parameter. The EFB model can also be simulated by Eq. (5) when R_b is replaced with R_f such that

$$\begin{aligned} g(r,b)&=1 \quad \text{for } r>R_f \\ &=\frac{1}{1+b^2 f(R_b)} \quad \text{for } r\leqslant R_f. \end{aligned} \tag{10}$$

In order to estimate the transmission, the action integral is calculated in two parts by integrating (i) from r_1 to R_f with a lower value of the effective reduced mass and (ii) from R_f to r_2 with the reduced mass having its normal value. Using the parabolic barrier approximation, the action integral between any two points x_1 and x_2 can be calculated as

$$\begin{aligned} S(x_1,x_2)=\frac{\beta\alpha^2}{2}\Bigg[&\sin^{-1}\left(\frac{x_2-R_l}{\alpha}\right)-\sin^{-1}\left(\frac{x_1-R_l}{\alpha}\right) \\ &+\frac{x_2-R_l}{\alpha}\sqrt{1-\left(\frac{x_2-R_l}{\alpha}\right)^2} \\ &-\frac{x_1-R_l}{\alpha}\sqrt{1-\left(\frac{x_1-R_l}{\alpha}\right)^2}\Bigg] \end{aligned} \tag{11}$$

with

$$\alpha^2=\frac{2(V_b-E)}{\mu\omega_l^2} \quad \text{and} \quad \beta=\frac{2\omega_l}{\hbar}\mu\sqrt{g(b)}. \tag{12}$$

It can be verified that when $x_1=r_1$ and $x_2=R_b$, the above result agrees with that of Eq. (4). Though we have two additional parameters $b_{\rm eff}$ and R_f, in order to simulate EFB we used a large value of the $b_{\rm eff}$ parameter. The results of the EFB model are also shown in the Figs. 1–4 (see curves labeled EFB). The R_f values needed for these four systems are 11.2 fm, 12.2 fm, 11.1 fm, and 12.5 fm, whereas the corresponding R_b values are 10.88 fm, 11.47 fm, 10.6 fm, and 11.71 fm. We have tried to fit the data up to the $\approx$0.1 mb

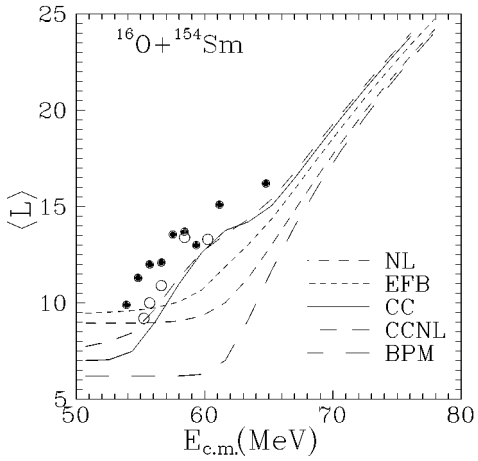

FIG. 5. $\langle L \rangle$ vs energy for the systems as given in Fig. 1.

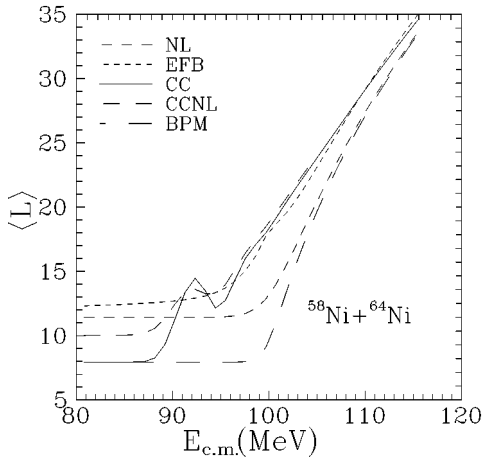

FIG. 7. $\langle L \rangle$ vs energy for the systems as given in Fig. 3.

level and the fits are quite satisfactory. The R_f values in all these cases come out to be larger than R_b, consistent with the results of Ref. [4]. We have compared the results of the BPM based on both nonlocal ion-ion potential (NL) and also the EFB model with the results of the dynamical coupled channel calculations using the standard local ion-ion potential. We have used the simplified coupled channel code CCFUS [11]. The various coupling parameters are given in the respective figure captions. It can be seen that the BPM with nonlocal effects cannot give a large enhancement as predicted by CC calculations (see curves NL and CC). In contrast, the EFB model with R_f as a parameter can be used to fit the fusion cross section for both above and a few MeV below the barrier. However, the results of the EFB model and the CC calculations differ significantly at deep subbarrier energies. Further, we have shown the energy dependence of the average spin $\langle L \rangle$ for these four systems in Figs. 5–8. It is important to note that the EFB calculations cannot reproduce the dynamical effects of CC calculations particularly around the barrier region. It may be noticed that neither NL nor EFB can reproduce the bump seen around the barrier region particularly for the deformed systems (see Fig. 5 and Fig. 6) . The curve NL strongly underestimates the experimental data, expected as it also underpredicts the fusion cross sections by several orders of magnitude. The predictions of the EFB and the CC calculations, which give similar cross section enhancements at and around the barrier region, differ significantly in the spin distribution. The EFB model results cannot reproduce the bump seen in the average spin values around the barrier energies. Further, the fusion enhancement arising due to the nonlocal effects cannot exceed the results of EFB. It is therefore important to realize that the EFB results provide an upper bound for results of any one-dimensional barrier penetration model.

In the case of the $^{58}Ni+^{64}Ni$ system, we have included a $2n$ transfer channel of Q value $+5$ MeV. This results in a peak in $\langle L \rangle$ around the barrier region (see Fig. 7) which is a characteristic feature of the couplings of positive Q value channels. Such a feature cannot be reproduced by the BPM with nonlocal effects. The curves labeled NL are quite close to the BPM results except for a different saturation value for $\langle L \rangle$. However, it is interesting to note that the EFB model results, although featureless around the barrier, are quite close to the experimental data. It can also be seen that the EFB model gives a much higher saturation value for $\langle L \rangle$ than the results from a simple CC calculation. Further, the coupled channel results cannot explain the large fusion cross section enhancement observed in the deep sub-barrier measurements of $^{19}F+^{232}Th$ system [9]. Therefore, the channel coupling effects are important around the barrier region whereas the nonlocal effects may give large fusion cross section enhancement at deep sub-barrier energies.

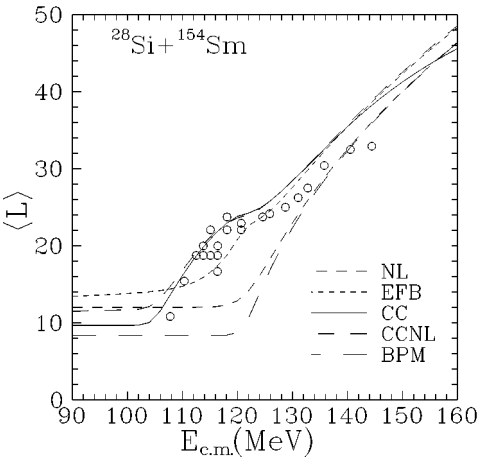

FIG. 6. $\langle L \rangle$ vs energy for the systems as given in Fig. 2.

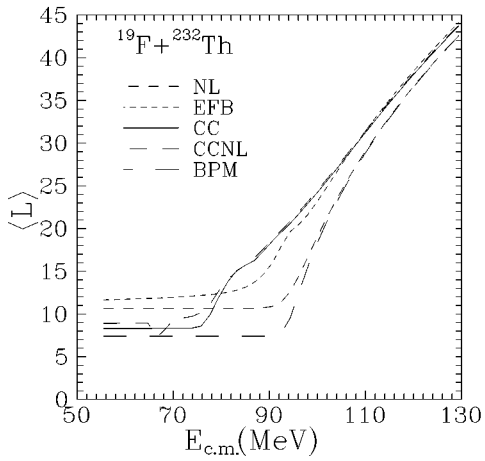

FIG. 8. $\langle L \rangle$ vs energy for the systems as given in Fig. 4.

III. COUPLED CHANNEL CALCULATIONS WITH NONLOCAL EFFECTS

In the above, we have shown that any BPM model with nonlocal potential or even the EFB model of Sahu and Shastry cannot reproduce the dynamical CC results. However, it is known that the basic ion-ion potential should be nonlocal and this aspect should be incorporated in any coupled channel calculation. Therefore, we carry out the coupled channel calculations with inclusion of nonlocal ion-ion potential as suggested by Galleti *et al.* [2], using the code CCFUS [11]. The transmission coefficient for fusion from different eigenchannels have been estimated using the barrier penetration model with a nonlocal ion-ion potential as discussed before, but using a realistic b parameter value of 2 fm [2]. It should be noted here that we have used a large $b_{\rm eff}$ value for the NL curve in order to maximize the nonlocal effects and also to obtain an upper bound on the fusion enhancements. In the case of coupled channel calculations, we aim at understanding the additional enhancement due to nonlocal effects with reasonable values of the b parameter. As seen before, the BPM model with (maximum) nonlocal effects (see the NL curve) does not account for experimental data of fusion enhancements. However, the coupled channel calculations with nonlocal effects (see CCNL) give the normal coupled channel results in the barrier region as well as a small enhancement at a deep sub-barrier region both for the fusion cross sections and its average spin values. These nonlocal effects may be of relevance at very low energies where normal CCFUS calculations fail to explain the experimental data (see experimental fusion cross section data for ^{19}F+^{232}Th system).

In coupled channel calculations, fusion is generally estimated either by using the WKB approximation for the transmission with an incoming wave boundary condition or by using an optical model with a short range imaginary potential. It is generally believed that both the methods will give similar results. However, recently we have shown that [14] the above two methods start deviating at low energies. This discrepancy becomes significant at very deep sub-barrier energies. The coupled channel formalism based on the optical model for fusion gives a higher estimate both for the fusion cross sections and its average spin values at deep sub-barrier energies. In the present study, we have used a coupled channel code based on the WKB approximation. More realistic codes like the ECIS and the FRESCO make use of optical model in order to evaluate transmission for fusion. As discussed in [14], these models are inherently different particularly at deep sub-barrier energies. Further, the use of nonlocal ion-ion potential can make the above difference more prominent. At this stage, it is difficult to say which effect is more important, however, this aspect should be kept in mind while analyzing the deep sub-barrier fusion data.

IV. CONCLUSION

In summary, we have analyzed the heavy ion fusion cross sections and the average spin values over a wide range of energies using the coupled channel calculations with a nonlocal ion-ion potential. The nonlocality has been incorporated by using an effective reduced mass as suggested by Galetti *et al.*. We showed that a simple barrier penetration model (BPM) with a nonlocal ion-ion potential is not enough to explain the fusion enhancement contrary to the claims of Galetti *et al.* and more recently by Dutt *et al.* Our results are in agreement with the predictions of the effective fusion barrier (EFB) model of Sahu and Shastry. The large fusion enhancement found by Galetti *et al.* and also by Dutt *et al.* is an artifact of the approximation made in the use of the reduced effective mass. These BPM results with nonlocal ion-ion potential and the results of the EFB model have been compared with the standard coupled channel calculations. It is shown that the BPM with nonlocal effects alone cannot give large fusion enhancements. In the case of the EFB model, it is possible to fit the fusion cross sections by using a suitable R_f parameter where $R_f > R_b$. However, both of these models cannot reproduce the characteristic features of the energy dependence of the spin distributions predicted by the dynamical coupled channel calculations. We have carried out simplified dynamical coupled channel calculations with a nonlocal ion-ion potential which explain fusion cross sections around the barrier region and show small enhancement at deep sub-barrier energies.

[1] A. K. Mohanty, S. V. S. Sastry, S. K. Kataria, and V. S. Ramamurthy, Phys. Rev. Lett. **65**, 1096 (1990); Phys. Rev. C **46**, 2102 (1992).

[2] D. Galetti and M. A. C. Ribeiro, Phys. Rev. C **50**, 2136 (1994); **51**, 1408 (1995).

[3] R. Dutt, T. Sil, and Y. P. Varshni, Phys. Rev. C **54**, 319 (1996).

[4] B. Sahu and C. S. Shastry, J. Phys. G **15**, L149 (1988).

[5] J. R. Leigh, M. Dasgupta, D. J. Hinde, J. C. Mein, C. R. Morton, R. C. Lemmon, J. P. Lestone, J. O. Newton, H. Timmers, J. X. Wei, and N. Rowley, Phys. Rev. C **52**, 3151 (1995).

[6] S. Gil, R. Vandenbosh, A. Charlop, A. Garcia, D. D. Leach, S. J. Luke, and S. Kailas, Phys. Rev. C **43**, 701 (1991).

[7] S. Gil *et al.*, Phys. Rev. Lett. **65**, 3100 (1990).

[8] R. A. Broglia, C. H. Dasso, S. Landowne, and G. Pollarolo, Phys. Lett. **133B**, 34 (1983).

[9] D. M. Nadkarni, A. Saxena, D.C. Biswas, R. K. Choudhury, S. S. Kapoor, N. Majumdar, and P. Bhattacharya (unpublished).

[10] P. R. Christensen and A. Winther, Phys. Lett. **65B**, 19 (1976).

[11] C. H. Dasso and S. Landowne, Comput. Phys. Commun. **46**, 187 (1987).

[12] N. Majumdar, P. Bhattacharya, D. C. Biswas, R. K. Choudhury, D. M. Nadkarni, and A. Saxena, Phys. Rev. C **54**, 3109 (1995).

[13] J. X. Wei, J. R. Leigh, D. J. Hinde, J. O. Newton, R. C. Lemmon, S. Elfstrom, J. X. Chen, and N. Rowley, Phys. Rev. Lett. **67**, 3368 (1991).

[14] S. V. S. Sastry, S. K. Kataria, A. K. Mohanty, and I. J. Thompson, Phys. Rev. C **54**, 3286 (1996).